

# Arsenic binding to organic and inorganic sulfur species during microbial sulfate reduction: a sediment flow-through reactor experiment

Raoul-Marie Couture,<sup>A,B,C,F</sup> Dirk Wallschläger,<sup>D</sup> Jérôme Rose<sup>E</sup>  
and Philippe Van Cappellen<sup>A,B</sup>

<sup>A</sup>Georgia Institute of Technology, 311 Ferst Drive, Atlanta, GA 30332, USA.

<sup>B</sup>University of Waterloo, 200 University Avenue West, Waterloo, ON, N2L 3G1, Canada.

<sup>C</sup>Norwegian Institute for Water Research, Gaustadalléen 21, N-0349 Oslo, Norway.

<sup>D</sup>Trent University, 1600 West Bank Drive, Peterborough, ON, K9J 7B8, Canada.

<sup>E</sup>CNRS-Aix Marseille University UMR 7330 CEREGE, Europôle de l'Arbois,  
13545 Aix-en-Provence, France.

<sup>F</sup>Corresponding author. Email: rmc@niva.no

**Environmental context.** The use of water contaminated with arsenic for drinking and irrigation is linked to water and food borne diseases throughout the world. Although reducing conditions in soils and sediments are generally viewed as enhancing arsenic mobility in subsurface environments, we show they can actually promote As sequestration in the presence of reduced sulfur species and labile organic matter. We propose that sulfurisation of organic matter and subsequent binding of As to thiol groups may offer an innovative pathway for As remediation.

**Abstract.** Flow-through reactors (FTRs) were used to assess the mobility of arsenic under sulfate reducing conditions in natural, undisturbed lake sediments. The sediment slices in the FTRs were supplied continuously with inflow solutions containing sulfate and soluble As<sup>III</sup> or As<sup>V</sup> and, after 3 weeks, also lactate. The experiment ran for a total of 8 weeks. The dissolved iron concentration, pH, redox potential ( $E_h$ ), as well as aqueous As and sulfur speciation were monitored in the outflow solutions. In FTRs containing surface sediment enriched in labile organic matter (OM), microbial sulfate reduction led to an accumulation of organically bound S, as evidenced by X-ray absorption spectroscopy. For these FTRs, the inflowing dissolved As concentration of 20  $\mu\text{M}$  was lowered by two orders of magnitude, producing outflow concentrations of 0.2  $\mu\text{M}$  monothioarsenate and 0.1  $\mu\text{M}$  arsenite. In FTRs containing sediment collected at greater depth, sulfide and zero-valent S precipitated as pyrite and elemental S, while steady-state outflow arsenite concentrations remained near 5  $\mu\text{M}$ . The observations thus suggest that As sequestration is enhanced when sediment OM buffers the free sulfide and zero-valent S concentrations. An updated conceptual model for the fate of As in the anoxic As–C–S–Fe system is presented based on the results of this study.

Received 18 January 2013, accepted 26 May 2013, published online 5 August 2013

## Introduction

Arsenic, a highly toxic metalloid, is a worldwide public health concern as As remobilisation from soil and sediment can contaminate water used for drinking and irrigation.<sup>[1–3]</sup> The high affinity of As for metal oxyhydroxides, in particular those of ferric iron, often leads to very low As concentrations in the aqueous phase at comparatively high solid phase concentrations. The latter nonetheless pose a threat as flooding, a rise in watertable or an increased supply of electron donors may create reducing conditions, which in turn may translocate As to the aqueous phase through a variety of processes, for instance microbial Fe<sup>III</sup> oxyhydroxide respiration coupled to the degradation of organic matter (OM).<sup>[3]</sup> Because under reducing conditions As can be sequestered by co-precipitation with,<sup>[4]</sup> or adsorption onto<sup>[5–7]</sup> Fe sulfides, such as pyrite (FeS<sub>2(s)</sub>) and mackinawite (FeS<sub>m(s)</sub>), production of sulfide as a result of microbial sulfate (SO<sub>4</sub><sup>2-</sup>) reduction has been suggested as a

possible As remediation pathway for subsurface environments.<sup>[8]</sup> The caveat, however, is that the redox boundary separating Fe<sup>III</sup> oxyhydroxides from Fe<sup>II</sup> and As sulfides is potentially a zone of high As remobilisation.

The environmental fate and transport of As is thus closely related to the biogeochemical cycling of iron, sulfur and carbon, as well as their relative abundances.<sup>[9–12]</sup> In reducing soils and sediments, in the presence of complex mineral assemblages,<sup>[13–16]</sup> As sorption onto Fe sulfides is often of minor importance except at high As loading and slightly acidic pH. Under the latter conditions, As uptake by Fe monosulfide (FeS<sub>m(s)</sub>) occurs through the formation of a sorption complex akin to realgar (AsS<sub>(s)</sub>), as shown by Gallegos et al.<sup>[17]</sup> In environments where all the reactive Fe is transformed into Fe sulfides, the remaining free sulfide (S<sup>-II</sup>) becomes available to complex As, allowing for the precipitation of As sulfide minerals, such as AsS<sub>(s)</sub> and orpiment (As<sub>2</sub>S<sub>3(s)</sub>), and the formation of

thiolated As species.<sup>[18]</sup> At the present time, the mechanisms by which aqueous S, including sulfide ( $S_{(aq)}^{-II}$ ), zero-valent sulfur ( $S_{(aq)}^0$ ) and polysulfides ( $S_n^0 S_{(aq)}^{-II}$ ), all ubiquitous in the aquatic environment,<sup>[19]</sup> promote thioarsenite and thioarsenate formation are not completely understood.<sup>[20]</sup>

The key influence of Fe and S on the geochemical behaviour of As has led to the classification of subsurface environments as exhibiting either Fe- or S-controlled As sequestration.<sup>[11]</sup> Because this classification does not explicitly consider the role of organic C – other than as an energy source for microbial metabolism<sup>[13,14]</sup> – it may overlook the full spectrum of reactions involving As and natural OM. For instance, it was recently shown that thiols (C–SH) present in OM-rich wetlands and peaty soils can efficiently bind arsenite.<sup>[21,22]</sup> Such geochemical conditions are likely not restricted to wetlands and may occur in other soils and sediments where thiols form as a result of assimilatory  $SO_4^{2-}$  reduction and OM sulfuration.<sup>[23]</sup> Nevertheless, although there is compelling evidence for the abundance of thiols, or reduced organic S ( $S_{org}$ ), in marine<sup>[24]</sup> and lake sediments,<sup>[25,26]</sup> thiol formation has so far been a neglected process in laboratory studies focussing on As mobility under sulfidic conditions. These studies typically only consider sulfide minerals as the dominant sink for reduced S.

Here, we used flow through reactors<sup>[27]</sup> (FTRs) containing undisturbed lake sediments to study As and S biogeochemistry under controlled, near steady state conditions. The FTR approach causes minimal disturbance of the physical and microbiological structure of the natural sediment and, hence, allows one to obtain information under environmentally relevant conditions. Our main objectives were to: (i) quantify the extent of thiol formation during microbial  $SO_4^{2-}$  reduction in aquatic sediments containing contrasting initial OM and Fe contents and (ii) identify the dominant aqueous and solid-phase As species formed during the microbially mediated formation of  $S_{(aq)}^0$ ,  $S_n^0 S_{(aq)}^{-II}$  and  $S_{(aq)}^{-II}$ , with a particular emphasis on organic and inorganic thiolated As.

The experimental design is illustrated in Fig. 1. The microbial community naturally present in the lake sediment samples

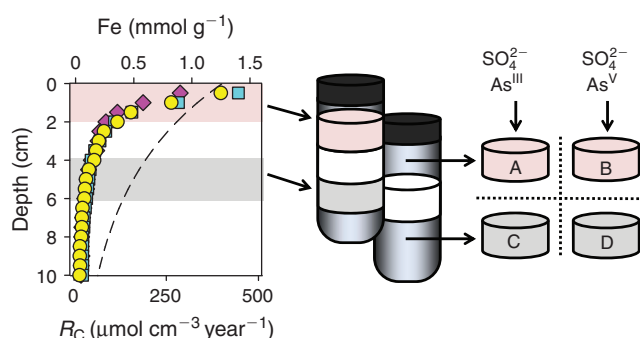


**Fig. 1.** Experimental design. The depth-profiles of Fe oxyhydroxides concentrations measured in 2003 (open circles), 2002 (open diamonds) and 1997 (open squares), and the depth distribution of organic carbon ( $C_{org}$ ) degradation rates measured in batch incubation ( $R_C$ ; dashed line) were used to select two depth intervals for the flow-through reactor (FTR) experiments.<sup>[26]</sup> Sediment from the 0–2-cm depth interval is enriched in Fe oxyhydroxides and labile organic matter relative to the deeper sediment. Also shown is a schematic representation of the sediment coring technique, which allows one to retrieve undisturbed sediment slices for use in the FTRs.<sup>[27]</sup> Note that FTR A and B were sourced from core #1 and FTR C and D from core #2 (see the *Field site and sediment sampling* section).

were stimulated by adding lactate and sulfate to induce microbial sulfidogenesis in four FTRs, two of them filled with the upper two centimetres of sediment from duplicate cores, and two with sediment from a deeper depth interval (4–6 cm). Sediment from the 0–2-cm depth interval was enriched in recently deposited (labile) OM, relative to the deeper sediment. The FTRs were supplied with solutions containing sulfate, and either dissolved  $As^{III}$  or  $As^V$ . After 3 weeks, the inflow solutions were further amended with a labile organic electron donor (lactate). The outflow solutions of the FTRs were analysed for dissolved constituents using a variety of analytical techniques, whereas solid-phase speciation of As and S were analysed by X-ray absorption spectroscopy (XAS).

## Methodology

### Field site and sediment sampling

Lake Tantaré (47°4'4"N, 71°32'59"W) is a slightly acidic (pH 5.8), perennially oxygenated ( $>3.75 \text{ mg O}_2 \text{ L}^{-1}$ ), oligotrophic headwater lake located in the Province of Québec, Canada. Three cores were collected by divers in September 2010 in the deepest, central part of the lake. Cores #1 and #2 supplied the sediment slices for the FTR, whereas core #3 was used to characterise the initial condition of the sediment. Sampling was carried out with shuttle corers<sup>[27]</sup> consisting of a continuous stacking of Plexiglas reactor cells. Once on shore, undisturbed sediment slices of 2-cm thickness and 4.7-cm diameter were recovered in an anaerobic glove bag (PE glove-bag, Alfa-Aesar, Ward Hill, MA, USA) purged with a continuous  $N_2$  flow. The FTRs were assembled within 30 min by placing nitrite (NBR) O-rings on the reactor cells, covering the sediment with 0.2- $\mu\text{m}$  pore size membranes (poly-ether sulfone, Pall Corporation, Port Washington, NY, USA), backing filters (fibreglass, Pall Corporation) and sealing the cells with high density polyethylene (HDPE) covers with input and output channels. The sealed FTRs were kept at 4 °C during shipment by plane from Québec City to the Georgia Institute of Technology in Atlanta, where the experiments were performed.

Sediments from the deepest part of Lake Tantaré have previously been shown to be laterally homogenous. The topmost sediment layer is enriched in diagenetic Fe oxyhydroxides ( $\sim 1 \text{ mmol Fe g}^{-1}$ , see Fig. 1),<sup>[26]</sup> consisting mainly of poorly crystalline ferrihydrite, lepidocrocite and goethite.<sup>[28]</sup> The sediments are organic-rich ( $\sim 20 \text{ mmol C}_{org} \text{ g}^{-1}$ ), with OM representing on average approximately half of the sediment's dry weight. The lability of sediment OM decreases exponentially with depth, as evidenced by the rates of  $C_{org}$  degradation ( $R_C$ ,  $\mu\text{mol C cm}^{-3} \text{ year}^{-1}$ ) measured independently in batch incubations.<sup>[26]</sup> The concurrent decrease of the concentration of Fe oxyhydroxides and of the lability of OM (Fig. 1) is attributed to OM degradation coupled to dissimilatory Fe reduction in the sediments,<sup>[26]</sup> a process that has been shown to induce profound changes in the reactivity of both OM and Fe oxyhydroxides over time.<sup>[29]</sup> Based on these expected differences in OM and Fe reactivity as a function of depth in the sediments, and on the previously determined depth profiles of solid-phase Fe and  $R_C$ , depth intervals 0–2 and 4–6 cm were selected for the FTR experiment. The uppermost sediments (0–2 cm), enriched in labile OM and in diagenetic Fe oxyhydroxides, are labelled FTRs A and B, whereas the deeper sediments (4–6 cm), depleted in labile OM and Fe oxyhydroxides (relative to the depth interval 0–2 cm) are labelled FTRs C and D.

## FTR experiments and aqueous phase characterisation

### General methods in the laboratory

Glass- and plastic-ware were cleaned by soaking in 10% (v/v) HNO<sub>3</sub> (VWR, ACS grade, Atlanta, GA, USA) for at least 24 h, followed by 24 h in 1% (v/v) HNO<sub>3</sub> and repeated rinsing with Milli-Q water (resistivity of 18.2 MΩ cm<sup>-1</sup>). Acids used for reagent solutions were of ultra-pure grade (VWR, Aristar grade), and all solutions were prepared using Milli-Q water, which was brought to boil and cooled while bubbling with high purity N<sub>2</sub>. As a precautionary measure, laboratory ware, (sealed) input solutions and coring equipment were sterilised by autoclaving or washing with an anti-bacterial agent.

### Experimental conditions

The experiment was conducted over 8 weeks (56 days) in an O<sub>2</sub>-free (2% H<sub>2</sub> in N<sub>2</sub> with O<sub>2(g)</sub> < 1 ppm) anaerobic chamber (Type A Vinyl Anaerobic Chamber with Pd catalyst, Coy Laboratories, Grass Lake, MI, USA). FTRs A and C were supplied with inflow solutions containing 20 μM of dissolved arsenate (NaHAs<sup>V</sup>O<sub>4</sub>·7H<sub>2</sub>O<sub>(s)</sub>; Sigma–Aldrich), whereas FTRs B and D were supplied with inflow solutions containing 20 μM of dissolved arsenite (Na<sub>2</sub>As<sup>III</sup>O<sub>2(s)</sub>; Sigma–Aldrich). All inflow solutions were made using 0.2-μm filtered deoxygenated Milli-Q water (see above) and contained 200 μM Na<sub>2</sub>SO<sub>4(s)</sub> (Alfa–Aesar). After 21 days, the inflow solutions to all FTRs were amended with 200 μM Na–lactate (Sigma–Aldrich) as an electron donor. Throughout the experiment, input solutions were adjusted to the lake's natural pH (5.8) and ionic strength (*I* = 0.5 mM) respectively using HCl–NaOH and NaCl (all Suprapur grade, EMD Chemicals). The solutions were supplied at an imposed constant flow rate of 1.0 ± 0.1 mL h<sup>-1</sup>, or ~1 pore volume day<sup>-1</sup>, using a peristaltic pump (ICP-N, Ismatec, Wertheim, Germany). The FTR outflows were collected in the anaerobic chamber using a computer-controlled fraction collector in vials containing, if needed, appropriate reagents for sample preservation (see below) and, unless otherwise noted, kept under N<sub>2</sub> until analysis. The following parameters were measured every two days in the FTR outflows: redox potential (*E<sub>h</sub>*), pH, [SO<sub>4</sub><sup>2-</sup>], total concentration of aqueous sulfides (ΣS<sup>-II</sup><sub>(aq)</sub>), total concentration of aqueous zero-valent S (ΣS<sup>0</sup><sub>(aq)</sub> = S<sup>0</sup><sub>(aq)</sub> + S<sup>0S</sup><sub>(aq)</sub>), total concentration of dissolved Fe and total dissolved As (ΣAs). Detailed aqueous As speciation was performed six times throughout the experiment, that is, every 7 days with the exception of day 35 where sample preservation could not be performed because of a liquid N<sub>2</sub> shortage. At the end of the FTR experiment the solid-phase was pressure-filtered under N<sub>2</sub>, homogenised and preserved in aliquots for analysis.

### Sample preservation

Samples for SO<sub>4</sub><sup>2-</sup> measurements were delivered to polypropylene tubes (Eppendorf) and those for major cations were delivered to 4-mL HDPE vials (VWR) containing 45 μL of 1.5 M HNO<sub>3</sub> (Aristar VWR); the tubes were kept at 4 °C until analysis. Samples for ΣS<sup>-II</sup> measurements were delivered to 4-mL PTFE-lined septa amber vials (VWR) containing 40 μL of 2.7 mM *N,N'*-dimethyl-*p*-phenylenediamine sulfate (Sigma–Aldrich) and 5.5 mM FeCl<sub>3</sub> (Alfa–Aesar). Samples for ΣS<sup>0</sup><sub>(aq)</sub> measurement were delivered to 4-mL PTFE-lined septa amber vials (VWR) containing 2 mL of double-distilled ethanol, 40 μL of tetrahydrofuran (THF, Sigma–Aldrich, HPLC grade), 0.4 mL of 1 M NaNO<sub>3</sub> (Merck, Suprapur grade), and 10 μL of

1 M HNO<sub>3</sub>. Samples for total As measurements were delivered to 3.5-mL HDPE vials (Camenco Cryovials), immediately flash-frozen in liquid N<sub>2</sub> and placed in a –80 °C freezer. The subset of samples selected for detailed aqueous As speciation was shipped overnight on dry-ice to Trent University (Canada), where the As speciation measurements were performed, and stored in a –80 °C freezer until analysis.

### Analytical techniques

The pH measurements were carried out in the anaerobic chamber using a gel-filled, epoxy-sealed electrode (VWR), and the redox potentials were measured using a 3.5 M KCl-filled Pt electrode (VWR) and converted into potential values relative to a standard hydrogen electrode. Dissolved concentrations of SO<sub>4</sub><sup>2-</sup> were analysed by ion chromatography (Dionex DX-300 system with AMMS-2 conductivity suppressor, IONPAC AG-14 column and AS-14 pre-column, Dionex Thermo-Fisher Scientific, Sunnyvale, CA, USA). Dissolved Fe concentrations were determined by inductively coupled plasma–optical emission spectroscopy (ICP-OES Ultima 2C, HORIBA Instruments, Chicago, IL, USA) and ΣS<sup>-II</sup><sub>(aq)</sub> by UV–Vis spectroscopy (DU Series 700, Beckman-Coulter, Atlanta, GA, USA). ΣS<sup>0</sup><sub>(aq)</sub> was analysed by square-wave cathodic stripping voltammetry (SW-CSV) in hanging Hg drop mode (Metrohm 940 VA Computrace, Metrohm USA, Riverview, FL, USA) according to Wang et al.<sup>[30]</sup> Total aqueous As concentrations were determined by atomic fluorescence spectroscopy coupled to continuous flow hydride generation (HG-AFS, PSA 10.055 Millennium Excalibur, PS Analytical, Orpington, UK). To eliminate the possibility of As sulfide precipitation within the flow-injection coil,<sup>[31]</sup> the pH of the sample was raised to pH > 10 with 1 N NaOH and then oxidised with 30% H<sub>2</sub>O<sub>2</sub> (VWR), thus oxidising As species to As<sup>V</sup> and S species to S<sup>VI</sup>.<sup>[32]</sup> The solid-bound C<sub>org</sub> and total sulfur (S<sub>tot</sub>) concentrations were determined on a CHNS analyzer (EA 1108, Carlo-Erba, Milan, Italy).

Aqueous As speciation was analysed by anion exchange chromatography (AEC, Dionex Thermo-Fisher Scientific) coupled to inductively coupled plasma–mass spectrometry (ICP-MS, Elan DRC II, Perkin-Elmer, Woodbridge, ON, Canada) according to Wallschläger and London.<sup>[33]</sup> Briefly, the separation was conducted at alkaline pH on a column with low hydrophobicity to allow intact and rapid elution of the acid-labile As–S compounds, and eluant elimination with a membrane suppressor was not used to prevent losses of certain methylated As species in the suppressor. Both As and S were measured as their oxides in dynamic reaction cell mode, using oxygen as the reaction gas. The following As species, shown in their completely deprotonated form (along with the abbreviation used for each throughout the manuscript), were separated: arsenite (AsO<sub>3</sub><sup>3-</sup>, As<sup>III</sup>), arsenate (AsO<sub>4</sub><sup>3-</sup>, As<sup>V</sup>), monothioarsenate (AsOS<sup>3-</sup>, MTAs<sup>V</sup>), dithioarsenate (AsO<sub>2</sub>S<sub>2</sub><sup>3-</sup>, DTAs<sup>V</sup>), trithioarsenate (AsOS<sub>3</sub><sup>3-</sup>, TTAs<sup>V</sup>), tetrathioarsenate (AsS<sub>4</sub><sup>3-</sup>, T<sub>4</sub>TAs<sup>V</sup>), monomethylarsenite ((CH<sub>3</sub>)AsO<sub>2</sub><sup>2-</sup>; MMAs<sup>III</sup>), monomethylarsenate ((CH<sub>3</sub>)AsO<sub>3</sub><sup>2-</sup>, MMAs<sup>V</sup>), monomethylmonothioarsenate ((CH<sub>3</sub>)AsSO<sub>2</sub><sup>2-</sup>, MMTAs<sup>V</sup>), monomethyldithioarsenate ((CH<sub>3</sub>)AsS<sub>2</sub>O<sup>2-</sup>, MMDTAs<sup>V</sup>), mono-methyltrithioarsenate ((CH<sub>3</sub>)AsS<sub>3</sub><sup>2-</sup>, MMTTAs<sup>V</sup>), dimethylarsenite ((CH<sub>3</sub>)<sub>2</sub>AsO, DMAs<sup>III</sup>), dimethylarsenate ((CH<sub>3</sub>)<sub>2</sub>AsO<sup>2-</sup>, DMAs<sup>V</sup>), dimethylmonothioarsenate ((CH<sub>3</sub>)<sub>2</sub>AsOS<sup>-</sup>, DMMTAs<sup>V</sup>) and dimethyldithioarsenate ((CH<sub>3</sub>)<sub>2</sub>AsS<sub>2</sub><sup>-</sup>, DMDTAs<sup>V</sup>). In addition, the total aqueous As concentration was determined independently by ICP-MS in the dynamic reaction cell mode, using oxygen as the reaction gas. The speciation mass balance (= Σ(detected As species)/(total As

concentration)) averaged  $107 \pm 18\%$  ( $1\sigma$ ) over all measured samples, confirming that all quantitatively significant As species were detected in the speciation analyses.

### Solid-phase characterisation

Solid-phase aliquots were collected from the sediment core #3 (initial conditions) as well as from each of the four reactors at the end of the experiment. Samples were either flash-frozen in liquid  $N_2$  and kept at  $-80^\circ C$  until XAS analysis or frozen at  $-20^\circ C$  until sequential extraction of S phases (see below).

Arsenic speciation in the sediment samples was examined by extended X-ray absorption fine structure spectroscopy (EXAFS) and by X-ray absorption near edge structure spectroscopy (XANES) at the As K-edge (11 867 eV) at the bending magnet beamline BM30b of the European Synchrotron Radiation Facility (ESRF, Grenoble, France). Sulfur speciation in the sediment samples was examined by XANES at the S K-edge (2472 eV) at the wiggler beamline 4-3 of the Stanford Synchrotron Radiation Laboratory (SSRL, Stanford, CA, USA). The X-ray energy resolution was achieved by a Si(111) monochromator calibrated relative to the L3-edge energy of an elemental gold ( $Au_{(s)}$ ) standard (Sigma-Aldrich) at 11 919 eV (As) or to the white line of a  $Na_2S_2O_3_{(s)}$  standard (Sigma-Aldrich) at 2479.3 eV (S). Spectra were collected in transmission mode using an ionisation chamber or in fluorescence mode using a 30-element array Canberra germanium solid-state detector (for As) or a 4-element solid-state Si detector (for S). Analyses for As were carried out at  $t < 15$  K in a helium (He) cryostat to limit As photooxidation or reduction, whereas those for S were carried with the sample compartment and detector under slight He over-pressure. For S, higher-order harmonics were reduced by detuning the second monochromator to 20% of its maximum intensity. Reference compounds were prepared as described in the Supplementary material.

For all edge-normalised, background corrected spectra, the relative contributions of the different As and S reference compounds were calculated by linear combination fitting (LCF) using the *ATHENA* software package.<sup>[34]</sup> The LCF procedure first aimed at reproducing quantitatively all the features of the spectra, using the smallest number of components, and removing those contributing to less than 5% of the sum. This step yielded fits with 1–3 components. Visually similar fits were further evaluated by selecting those with the lowest *R*-factor values, and permutations were tested by selecting the combinations that lowered the reduced Chi-square ( $\chi^2_{red}$ ) values by at least 20%, which was deemed a significant improvement. The suite of reference materials included was as follows: (i) the sodium salts of  $As^{III}$  and  $As^V$  (Sigma-Aldrich),  $MTAs^V$  and  $TTAs^V$  prepared according to Wallschläger and Stadey,<sup>[35]</sup> (ii) the minerals  $AsS_{(s)}$  (Sigma-Aldrich),  $As_2S_3_{(s)}$  (Alfa-Aesar), nano-crystalline  $As_2S_3_{(s)}$  (digitised from Helz et al.<sup>[36]</sup>), scorodite and arsenopyrite (D. Testemale, pers. comm. and James-Smith et al.<sup>[37]</sup>), (iii) the sorption complexes of  $As^{III}$ ,  $As^V$ ,  $MTAs^V$  and  $TTAs^V$  sorbed onto two-lines ferrihydrite, goethite,  $FeS_{m(s)}$  and  $FeS_{2(s)}$  (Couture et al.<sup>[38]</sup>) and (iv) the thiol-bound  $As^{III}$  species glutamyl-cysteinyl-glycinylothioarsenite ( $As^{III}$ -glu; C. Mikutta, pers. comm and Langner et al.<sup>[21]</sup>). For S K-edge XANES, the suite of reference material included was as follows:  $FeS_{2(s)}$  (Strem Chemicals), rhombic elemental sulfur ( $S(\alpha)_{8(s)}$ ; Alpha-Aesar), cysteine ( $S_{cyst}$ ; Sigma-Aldrich), methionine sulfoxide (Sigma-Aldrich), cysteic acid (Sigma-Aldrich) and chondroitin sulfate (Sigma-Aldrich). To

determine changes in solid-phase S composition over the course of the experiment, initial lake sediment samples from the two depth intervals were included with the reference compounds.

Despite precautions taken during sample preparation, S K-edge XANES can display non-linear additive behaviour depending on the S content and particle size distribution of the sample,<sup>[39]</sup> thus introducing uncertainty in the LCF estimations. To complement the XANES results, three inorganic solid-phase S pools were therefore operationally defined based on the classic sequential extraction scheme for acid-volatile sulfide (AVS), chromium-reducible sulfur (CRS) and elemental sulfur (ES), and nominally ascribed to the species  $FeS_{m(s)}$ ,  $FeS_{2(s)}$  and  $S(\alpha)_{8(s)}$ . The extraction scheme chosen, detailed in the Supplementary material, was optimised for room temperature and is safer than protocols involving heated acidic oxidising solutions.<sup>[40,41]</sup> Sulfur not released by the sequential extraction scheme was assumed to represent organic S ( $S_{org} = S_{tot} - [AVS + CRS + ES]$ ). Note that we elected not to apply sequential extractions for As and Fe because the outcomes of published extraction schemes in the presence of reduced S species have been criticised.<sup>[10]</sup>

### Thermodynamic calculations

Thermodynamic calculations were performed with the public domain computer code PHREEQC, Version 2.17.5.<sup>[42]</sup> To be used with PHREEQC,  $E_h$  values were converted into *pe* (negative logarithm of the hypothetical electron activity) using the Nernst Equation ( $E_h = 0.059 \times pe$ ). The following calculations were performed: (i) the theoretical *pe* based on the ratios of the measured redox couples and (ii) the saturation state of the FTR outflows with respect to selected sulfur minerals ( $AsS_{(s)}$ ,  $As_2S_3_{(s)}$ ,  $AsFeS_{(s)}$ ,  $FeS_{(s)}$ ,  $FeS_{m(s)}$ ,  $FeS_{t(s)}$ ,  $FeS_{2(s)}$  and  $\alpha S_{8(s)}$ ). Details on the thermodynamic calculations and databases used are given in the Supplementary material.

## Results

### Solid phase transformations during FTR experiments

The quantity and speciation of S sequestered in the FTRs over the course of the experiment differed strikingly between the 0–2- and 4–6-cm depth intervals. FTRs A and B (0–2 cm, OM respiration rates  $\sim 600 \mu mol C g^{-1} year^{-1}$ ) sequestered 80 and  $87 \mu mol S g^{-1}$ , whereas FTRs C and D (4–6 cm, OM respiration rates  $\sim 65 \mu mol C g^{-1} year^{-1}$ ) sequestered 35 and  $53 \mu mol S g^{-1}$ . Both the sequential extractions and LCF of XANES spectra at the S K-edge (Table 1 and Fig. 1) implied that the majority of S accumulated in FTRs A and B was in the reduced  $S_{org}$  fraction (estimated by LCF using cysteine as a reference compound), whereas most S accumulated in the  $FeS_{2(s)}$  and  $S(\alpha)_{8(s)}$  fractions in FTRs C and D. Negative values of AVS (Table 1) indicate that they represented a smaller proportion of total S after the incubation than in the initial sediment.

Of the 26 reference compounds considered, six were necessary for the LCF procedure to reproduce the As K-edge XAS spectra of the entire set of samples (Table 2 and Fig. 2b–c). The positions of the As K-edge XANES peaks indicate that As accumulated predominantly as  $As^{III}$  in the FTRs (Table 2). In FTRs A and B, 45% of solid-phase As was attributed to  $AsS_{(s)}$ , 35–45% to thiol-bound As ( $As^{III}$ -glu) and the remaining to As sorbed onto goethite initially present in the 0–2-cm depth interval sediment. The high proportion of  $AsS_{(s)}$  in FTRs A and B (Table 2) is compatible with the observation that almost all S is under the organic form (Table 1), because mass-balance

**Table 1. Solid-phase speciation of S (as a percentage of total S) accumulated by the sediments in the flow-through reactors (FTRs) during the experiment**

The percentages were estimated by the difference between final and initial concentrations in the case of sequential extractions or by linear combination fitting (LCF) of normalised X-ray absorption near edge structure (XANES) spectra at the S K-edge using the initial samples as components of the fit. The mean-square misfits between measured and modelled XANES data (*R* factor) are also given. *R* factor =  $(\sum(\text{data-fit})^2)/(\sum(\text{data})^2)$ ; lower values indicate better goodness of fit. AVS, acid-volatile sulfide; CRS, chromium-reducible sulfur; ES, elemental sulfur;  $S_{\text{org}}$  (organic S), total S – [AVS + CRS + ES];  $\text{FeS}_{\text{m(s)}}$ , mackinawite;  $\text{FeS}_{2(\text{s})}$ , pyrite;  $S(\alpha)_{8(\text{s})}$ , elemental sulfur;  $S_{\text{cyst}}$ , cysteine

FTR	Sequential extractions				LCF				<i>R</i> factor
	AVS	CRS	ES	$S_{\text{org}}$	$\text{FeS}_{\text{m(s)}}$	$\text{FeS}_{2(\text{s})}$	$S(\alpha)_{8(\text{s})}$	$S_{\text{cyst}}$	
A	+4	7	8	81	–	<5	<5	95	0.0091
B	+5	1	2	92	–	<5	<5	95	0.0087
C	–3	89	23	–	–	100	–	–	0.0068
D	–3	42	36	25	–	55	45	–	0.0040

**Table 2. Solid-phase speciation of As (as a percentage of total As) accumulated by the sediments in the flow-through reactors (FTRs) during the experiment**

The percentages were estimated using linear combination fitting (LCF) of normalised As K-edge extended X-ray absorption fine structure (EXAFS) spectra. The mean-square misfits between measured and modelled EXAFS data (*R* factor) are also given. *R* factor =  $(\sum(\text{data-fit})^2)/(\sum(\text{data})^2)$ ; lower values indicate better goodness of fit.  $\text{AsS}_{(\text{s})}$ , realgar;  $\text{As}_2\text{S}_3(\text{s})$ , orpiment; geo, goethite;  $\text{As}^{\text{III}}\text{-glu}$ , glutamyl-cysteinyl-glycyl-thioarsenite;  $\text{As}^{\text{V}}\text{S}_4$ , tetrathioarsenate

FTR	LCF						<i>R</i> factor
	$\text{AsS}_{(\text{s})}$	$\text{As}_2\text{S}_3(\text{s})$	$\text{As}^{\text{V}}$ ( $\equiv$ goe)	$\text{As}^{\text{III}}$ ( $\equiv$ goe)	$\text{As}^{\text{III}}\text{-glu}$	$\text{As}^{\text{V}}\text{S}_4$	
A	45	–	20	–	35	–	0.043
B	45	–	–	10	45	–	0.037
C	30	35	–	–	–	35	0.039
D	35	40	–	25	–	–	0.052

calculations indicate that  $\text{AsS}_{(\text{s})}$  contributes, at most, to 3% of the total S, a proportion lower than the precision of  $\pm 5\%$  typically afforded by LCF procedures. For the deeper sediments (FTRs C and D), the dominant As species was identified as  $\text{As}_2\text{S}_3(\text{s})$ . In FTR C, LCF suggests that an  $\text{As}^{\text{V}}\text{-S}$  compound (using  $\text{TTAs}^{\text{V}}$  as a reference material) contributed on the order of 35% of the total As.  $\text{FeAsS}_{(\text{s})}$ , as well as  $\text{As}^{\text{III}}$  and  $\text{As}^{\text{V}}$  sorbed onto  $\text{FeS}_{\text{m(s)}}$  or  $\text{FeS}_{2(\text{s})}$ , which were previously shown to produce distinctly different EXAFS spectra than either  $\text{As}^{\text{III}}\text{-glu}$ ,  $\text{AsS}_{(\text{s})}$  or  $\text{As}_2\text{S}_3(\text{s})$ ,<sup>[4,21]</sup> were included in the LCF procedure, but were not found to contribute to the samples' fluorescence.

#### Aqueous chemistry of the FTR outflows

Concentration time-series of the outflows of the FTRs are shown in Fig. 3. The first 21 days are referred to as the 'acclimation phase' and the period from day 36 till the end of the experiment (day 56), during which the concentrations of  $\text{SO}_4^{2-}$  in the outflows of all FTRs reached near constant values of  $\sim 2\ \mu\text{M}$ , is referred to as the 'steady state phase'. During the acclimation phase, FTRs A and B consumed  $\text{SO}_4^{2-}$  faster than FTRs C and D. After  $\sim 15$  days, outflow  $\text{SO}_4^{2-}$  concentrations levelled off for FTRs C and D, but they started to increase for FTRs A and B,

indicating that  $\text{SO}_4^{2-}$ -reducing microorganisms were depleting the readily available OM pool. We then added lactate, a substrate known to stimulate sulfate-reducing microorganisms,<sup>[15,43]</sup> to the inflowing solutions on day 21. Outflow  $\Sigma\text{S}_{(\text{aq})}^0$  concentrations were systematically lower in FTRs A and B, compared with FTRs C and D. Upon the addition of lactate,  $\Sigma\text{S}_{(\text{aq})}^0$  in FTRs A and B peaked briefly to  $3.5\ \mu\text{M}$  and then returned to  $1\text{--}2\ \mu\text{M}$ , whereas in FTRs C and D  $\Sigma\text{S}_{(\text{aq})}^0$  increased to  $7\text{--}17\ \mu\text{M}$  for 12 days before dropping to values in the range of  $2\text{--}5\ \mu\text{M}$ .

Outflow  $\Sigma\text{S}^{-\text{II}}$  was the only aqueous species that showed systematic differences between the  $\text{As}^{\text{III}}$  and the  $\text{As}^{\text{V}}$ -fed FTRs, being higher for  $\text{As}^{\text{V}}$  (FTRs B and D) than for  $\text{As}^{\text{III}}$  (FTRs A and C) by  $\sim 5\ \mu\text{M}$ . Outflow  $\Sigma\text{S}_{(\text{aq})}^{-\text{II}}$  concentrations in FTRs B and D remained comparatively low, between  $0.5$  and  $5\ \mu\text{M}$ , throughout the experiment, whereas in FTRs A and C they increased steadily during the acclimation phase, plateaued at  $10\text{--}12\ \mu\text{M}$  after the addition of lactate, and decreased slightly towards the end of the experiment. The outflow Fe concentrations were higher for the  $0\text{--}2\text{-cm}$  depth interval sediment FTRs (A and B), reaching values up to  $10\ \mu\text{M}$  during the acclimation phase and remaining at  $\sim 5\ \mu\text{M}$  during the steady state phase. In comparison, Fe concentrations remained  $< 1\ \mu\text{M}$  for the  $4\text{--}6$  depth interval sediment FTRs (C and D) throughout the experiment.

Outflow  $\Sigma\text{As}$  concentrations increased progressively at the beginning of the experiments, peaking at  $\sim 15\ \mu\text{M}$  on day 20 (Fig. 3). They decreased abruptly for all FTRs upon lactate addition. Towards the end of the experiment,  $\Sigma\text{As}$  was an order of magnitude lower in the outflows of FTRs A and B than in those of FTRs C and D, with average values of  $\sim 0.5$  and  $\sim 5.0\ \mu\text{M}$ . Aqueous As speciation analyses (Fig. 3) revealed measurable quantities of methylated-As species (limits of detection (LODs) of  $\sim 2\ \text{nmol L}^{-1}$  for As and  $50\ \text{nmol L}^{-1}$  for S), with  $\text{MMAs}^{\text{V}}$  being the most abundant. Only  $\text{As}^{\text{III}}$ ,  $\text{As}^{\text{V}}$ ,  $\text{MTAs}^{\text{V}}$  and  $\text{DTAs}^{\text{V}}$  represented  $> 2\%$  of the total outflowing dissolved As concentration at any given time. Irrespective of the oxidation state of As in the input solutions, the outflows contained between 75 and 25%  $\text{As}^{\text{V}}$  during the acclimation phase and  $\sim 25\%$   $\text{As}^{\text{V}}$  during the steady state phase (Fig. 3 and Table S1). Thiolated-As species were more abundant in the outflows of FTRs A and B, with  $\text{MTAs}^{\text{V}}$  representing  $\sim 25\%$  of the total dissolved As during the first week of the experiment, decreasing to  $1\text{--}2\%$  towards the end of the acclimation phase, and increasing again during the steady state phase. At the end of the experiment,  $\text{MTAs}^{\text{V}}$  concentrations reached  $12.4\ \mu\text{M}$  in FTR A and  $13.1\ \mu\text{M}$  in FTR B, becoming the dominant aqueous As species in the  $0\text{--}2\text{-cm}$  depth interval sediment FTR supplied with  $\text{As}^{\text{III}}$  (FTR A) representing 32% of the total dissolved As leaving the reactor.

## Discussion

### Sinks for reduced sulfur during microbial sulfate reduction

The sediments in FTRs C and D sequestered S as  $\text{FeS}_{2(\text{s})}$  and  $S(\alpha)_{8(\text{s})}$  (Table 1), in line with recent studies on microbial sulfidogenesis in soils, sediments and laboratory columns reporting that these S species are the primary end products of  $\text{SO}_4^{2-}$  reduction.<sup>[13,14,24,44]</sup> A possible mechanism for the accumulation of elemental S in the sediments is its precipitation from  $\text{S}_{(\text{aq})}^0$  produced during the oxidation of  $\text{S}_{(\text{aq})}^{-\text{II}}$  by Fe oxyhydroxides.<sup>[45]</sup> Thermodynamic calculations indicate that  $S(\alpha)_{8(\text{s})}$  was oversaturated by 0.5–2 orders of magnitude (saturation index =  $\log \text{IAP}/K_{\text{sp}}$  where IAP is the ion activity product

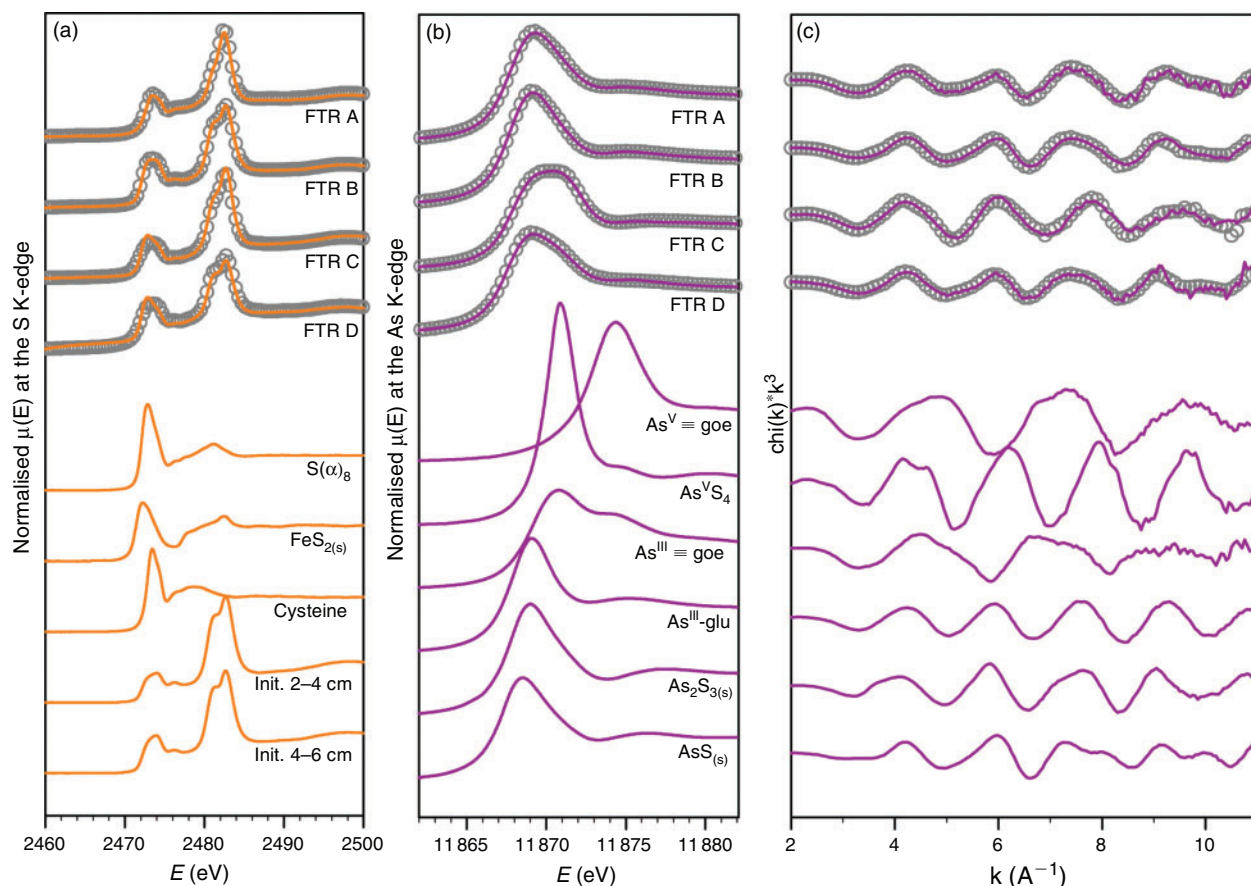


**Fig. 2.** Relative absorbance of normalised spectra at the S K-edge (panel A), and of normalised spectra (panel B) and  $k^3$ -weighted extended X-ray absorption fine structure (EXAFS) spectra (panel C) at the As K-edge for flow-through reactor (FTR) samples collected at the end of the experiment, reference compounds and initial sediment (panel A). Solid lines indicate experimental data and open circles the corresponding best linear combination fits. See main text for definitions of the different types of As and S species indicated.

and  $K_{sp}$  is the solubility product) in the outflow of all FTRs throughout the experiment.

In the surface sediments (0–2 cm, FTRs A and B), the results suggest that the dominant sink for  $S_{(aq)}^{-II}$  and  $S_{(aq)}^0$  produced as a result of microbial sulfate reduction is thiol formation (Table 1). Sulfurisation of OM as a sink for reduced S species has been observed in natural environments, and has been proposed to be a key early diagenetic process in sediments overlain by sulfidic waters.<sup>[23]</sup> The dominance of thiol formation in the upper 2 cm of sediment is likely related to the presence of labile OM, which is needed both as a substrate to support bacterial  $SO_4^{2-}$  reduction and as a reactant for  $S_{(aq)}^{-II}$  and  $S_{(aq)}^0$  to form thiols.<sup>[46]</sup> The observation that outflow Fe concentrations in FTRs A and B are an order of magnitude higher than in the outflow of FTRs C and D (Fig. 3) suggests that Fe is outcompeted by OM as a sink for reduced S. In addition, lower outflow  $S_{(aq)}^{-II}$  concentrations in FTRs B and D than in FTRs A and C are consistent with the observation that the former FTRs accumulated more solid-phase S than the latter FTRs during the incubations (see the *Solid phase transformations during FTR experiments* section). This difference in the  $S_{(aq)}^{-II}$  dynamic between  $As^{III}$  and  $As^V$ -fed FTRs may be due to a greater affinity of  $S_{(aq)}^{-II}$  for  $As^V$  than for  $As^{III}$ , consistent with the current best estimates of the free energy values for the sulfidation of these As species.<sup>[47]</sup>

Sulfurisation of OM has mostly been studied in marine sediments, where it is typically slower than the formation of Fe sulfides and occurs over time scales of  $10^2$ – $10^4$  years.<sup>[46]</sup> In

contrast, in this study with freshwater lake sediments, thiols form on time scales of days to weeks, most likely as a result of a combination of factors, such as the high rates of sulfate reduction and the nature of the labile OM deposited from the water column. One hypothesis worth further investigation is that soil-derived OM in lake sediments may be promoting fast thiol formation because of its high content of oxidised S (up to 98 % total  $S_{org}^{[48]}$ ), mainly in the form of easily hydrolysable ester- $SO_4^{[25,49]}$  or sulfonate.<sup>[50]</sup>

#### Controls on As mobility

XAS results show that As sorbed onto Fe oxyhydroxides is present at the end of the experiment (Table 2), suggesting incomplete sulfidation of the Fe oxyhydroxides. Consistent with previous reports,<sup>[13,14,16]</sup> we see no evidence for extensive As adsorption onto Fe sulfides in the FTRs. LCF does suggest, however, the formation of  $AsS_{(s)}$ , despite the fact that the outflow of all FTRs is undersaturated by >2 orders of magnitudes with respect to  $AsS_{(s)}$ . This apparent contradiction has been previously reported at circum-neutral pH<sup>[15]</sup> and can be ascribed to a surface reaction of As onto Fe sulfides which lead to a local As coordination that, using XAS, is indistinguishable from an  $AsS_{(s)}$ -like solid phase.<sup>[6,7,12,17,51]</sup>

In the FTRs A and B, where thiol formation was the dominant sink for reduced S, LCF suggests that thiol-bound  $As^{III}$  accounts for a third of the total As. The sequestration of  $As^{III}$  by organic S moieties of natural OM through the formation of thiol-bound As

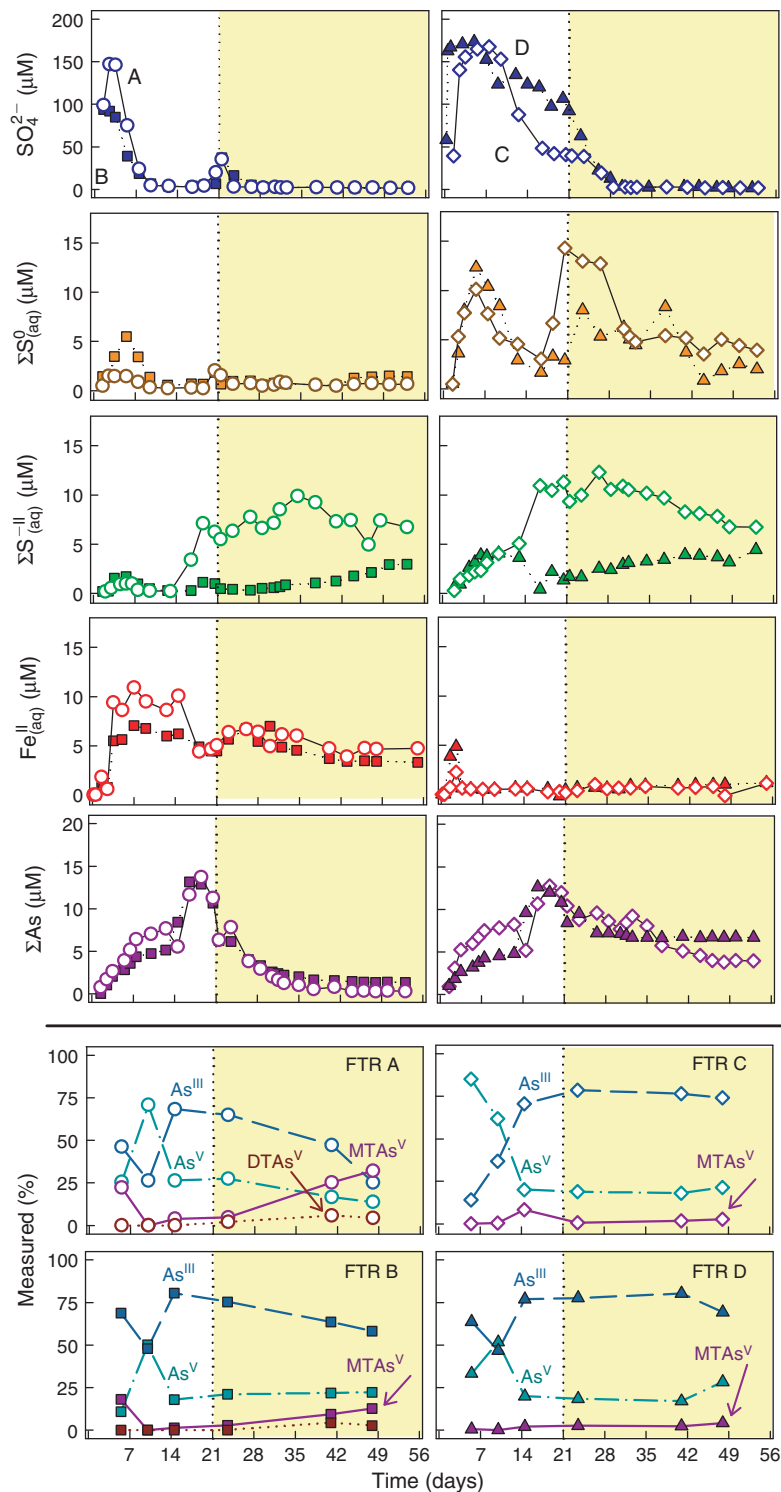


**Fig. 3.** Concentrations of dissolved  $\text{SO}_4^{2-}$ ,  $\Sigma\text{S}^0_{(\text{aq})}$ ,  $\Sigma\text{S}^{\text{II}}_{(\text{aq})}$ ,  $\text{Fe}^{\text{II}}_{(\text{aq})}$  and  $\Sigma\text{As}$  in the outflows of flow-through reactors (FTRs) A (circles), B (squares), C (diamonds) and D (triangles) (upper panels), and relative abundances of  $\text{As}^{\text{III}}$  (thick dashed line),  $\text{As}^{\text{V}}$  (dashed-dotted line), monothioarsenate ( $\text{MTAs}^{\text{V}}$ , thick solid line) and dithioarsenate ( $\text{DTAs}^{\text{V}}$ , thick dotted lines) (lower panels); species with an abundance of  $<2\%$  were omitted for clarity. Open and solid symbols respectively denote FTRs supplied with  $\text{As}^{\text{III}}$  and  $\text{As}^{\text{V}}$ . The shaded areas indicate the period during which the FTRs were supplied with lactate.

has been reported only very recently in peat samples.<sup>[21,22]</sup> To our knowledge, this process has never before been demonstrated in controlled experiments with sediments. For peat, Langner et al.<sup>[21]</sup> hypothesised that  $\text{As}^{\text{III}}$  complexation by freshly formed

thiol, or the reaction of thiolated-As directly with OM, is a dominant sink for As during sulfate reduction. According to these authors, LCF of As K-edge EXAFS spectra is able to discriminate between  $\text{As}_2\text{S}_3(\text{s})$ , both crystalline and nano-crystalline,

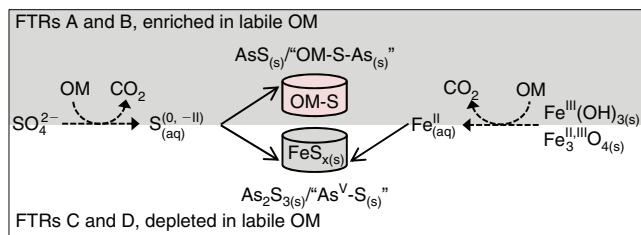


**Fig. 4.** Conceptual model of the formation of As–S species under anoxic conditions. The dominant As species formed through each pathway are indicated in bold. Solid lines indicate the formation of a complex, covalent bond or precipitate; dashed lines indicate organic matter (OM) oxidation reactions. See main text for definitions of the different types of As and S species indicated.

and  $\text{As}^{\text{III}}$  coordinated to thiol. They used Morlet wavelet analysis to show that a spectroscopic feature of the  $\text{As}_2\text{S}_{3(s)}$  spectra, characteristic of As backscattering, is absent from the spectra of As–thiol compounds. Although evidence based solely on LCF is not definitive, the results presented here provide further grounds for more detailed investigations of thiol-formation as an As sequestration pathway.

In FTR C, LCF suggests the presence of an  $\text{As}^{\text{V}}\text{-S}$  bond, based on  $\text{TTAs}^{\text{V}}$  as a reference compound (Fig. 1). The presence of  $\text{As}^{\text{V}}\text{-S}$  is supported by the analysis of the EXAFS data using Fourier transform (see Fig. S1), revealing that the average As–S bond distances (uncorrected for backscattered phase shift) in this sample is equal to the previously reported value for  $\text{As}^{\text{V}}\text{-S}$ ,<sup>[18]</sup> which is  $\sim 0.10$  Å shorter than for  $\text{As}^{\text{III}}\text{-S}$ . However, based on our current understanding of the geochemistry of  $\text{TTAs}^{\text{V}}$ , it is doubtful that it is formed in FTR C, because  $\text{TTAs}^{\text{V}}$  is unstable at  $\text{pH} < 10$ .<sup>[52]</sup> Indeed,  $\text{TTAs}^{\text{V}}$  was not detected in the outflow of any the FTRs. Instead, other species such as di- or tri-thioarsenate are potentially present, both being stable at circumneutral pH and likely to form in FTR C which produced the highest outflow  $\Sigma\text{S}^{-\text{II}}$  and  $\Sigma\text{S}^0_{(aq)}$  concentrations (Fig. 2). The presence of these S species are thought to promote  $\text{As}^{\text{III}}$  oxidation and sulfidation<sup>[35,47,53]</sup> through an electrophonic addition of an  $\text{S}^0$  atom to the free electron pair of  $\text{As}^{\text{III}}$ ,<sup>[35]</sup> yielding an  $\text{As}^{\text{V}}\text{-S}$  complex.

In all FTRs, the outflow  $\Sigma\text{As}$  concentrations peaked during the transition period separating maximum aqueous Fe and maximum  $\Sigma\text{S}^{-\text{II}}_{(aq)}$  concentrations (Fig. 3). High As mobility at this redox transition has been previously ascribed to the time lag between the onset of reductive dissolution of Fe oxyhydroxides, to which As is likely sorbed, and that of free sulfide accumulation in the pore water, which ultimately lead to the precipitation of As sulfide phases.<sup>[11]</sup> During this transition, the aqueous As in the FTR outflows progresses from equal proportions of  $\text{As}^{\text{V}}$  and  $\text{As}^{\text{III}}$  towards the predominance of  $\text{As}^{\text{III}}$ , irrespective of what As species is supplied with the inflow (Fig. 3). Arsenic speciation evolves towards higher proportions of  $\text{MTAs}^{\text{V}}$  in all FTRs, becoming the dominant dissolved As species in the outflow of FTR A by the end of the experiment. Aqueous As speciation thus appears to be closely controlled by the biogeochemical conditions established in the FTRs, driven by the microbial community utilising S, and likely also Fe and As as energy sources. Calculation of the theoretical  $pe$  (Fig. S1) using the  $\text{SO}_4\text{-HS}^-$ ,  $\text{S}^0_{(aq)}\text{-HS}^-$ ,  $\text{As}^{\text{III}}\text{-As}^{\text{V}}$  and  $\text{Fe}^{\text{II}}_{(aq)}\text{-Fe}^{\text{III}}(\text{OH})_3_{(s)}$  redox couples reveal that only the  $pe$  values calculated using the  $\text{S}^0_{(aq)}\text{-HS}^-$  redox couple remained within 1  $pe$  unit of the

measured values, suggesting, as previously hypothesised,<sup>[47,53]</sup> that this couple may be the effective redox buffer controlling As speciation (Fig. S2).

#### Conceptual model for As sequestration in sulfidic sediment

In the reactors containing the topmost sediment (FTRs A and B), the formation of thiols appears to be the primary sink for sulfides and other reduced S species produced by microbial  $\text{SO}_4^{2-}$  reduction. This leads to enhanced As sequestration through the formation of  $\text{AsS}_{(s)}$  (or of an analogue surface precipitate) and thiol-bound  $\text{As}^{\text{III}}$ , suggesting that thiol formation, resulting from OM sulfuration, could be used as a remediation pathway for metalloids such as As. In the FTRs with the deeper sediment (FTRs C and D), which presumably contained less labile OM,<sup>[26]</sup> the dominant sink for sulfides is the formation of Fe-minerals and elemental S. The remaining sulfides are available to complex As and form As sulfide minerals. We also observed the formation of thiolated  $\text{As}^{\text{V}}$  species, both in the aqueous and in the solid phase, despite the reducing conditions. In the aqueous phase, all FTRs produced  $\text{MTAs}^{\text{V}}$ , a species not observed before in pore waters of sulfidic sediments. The biogeochemistry of  $\text{MTAs}^{\text{V}}$  is currently under intense scrutiny because of its mobility,<sup>[54]</sup> kinetic stability<sup>[55]</sup> and possible innocuity.<sup>[56,57]</sup> Thus, the sequestration of As and the concomitant mobilisation of small quantities of  $\text{MTAs}^{\text{V}}$  represent a scenario where both sequestration and potential detoxification of As contribute to reducing the risk of As contamination.

Based on these results, we propose an updated conceptual model for the fate of As in OM-rich sediments, which includes the role of OM as a sink for S and its control on As sequestration through the formation of thiol-bound  $\text{As}^{\text{III}}$  (Fig. 4). This model complements the generally accepted idea that Fe is the effective buffer for  $\text{S}^{-\text{II}}$  produced during  $\text{SO}_4^{2-}$  reduction, and the current classification of As sequestration in sediments as being either Fe- or S-controlled.<sup>[11]</sup> The implications of the prevalence of thioarsenates and thiol-bound As species for the mobility and remediation of As, and thus for the quality of the water used worldwide for drinking and irrigation, are significant. The stimulation of thiol formation through microbial sulfidogenesis has yet to be considered as a pathway of remediation for metalloids in the subsurface, which could be relevant for aquifers subjected to naturally high levels of sediment-bound As, such as those of South-east Asia.<sup>[2]</sup>

#### Acknowledgements

The authors thank D. Campisi, J. Evans, N. Kumar, K. Mitchell and M. Trail for research assistance in the field and in the laboratory. They acknowledge the ESRF for provision of synchrotron facilities and thank D. Testemale for assistance at the FAME beamline BM30b. A portion of this research was performed at SSRL, a user facility supported by the US Department of Energy, Office of Sciences; the authors thank E. Nelson for assistance at beamline 4–3. They are indebted to C. Mikutta (ETH, Switzerland) for providing the reference spectrum of  $\text{As}^{\text{III}}\text{-glu}$  and to D. Testemale (ESRF) and J. Brugger (University of Adelaide) for the reference spectrum of scorodite and arsenopyrite. Logistical support from C. Gobeil and R. Rodrigue (INRS-ETE) and permission to work in the Tantaré Ecological Reserve granted by the Québec MEDDEP is gratefully acknowledged. K. Mueller kindly accepted to edit the manuscript. R.-M. Couture was financially supported by a postdoctoral fellowship from the Fonds de recherche du Québec – Nature et technologies. P. Van Cappellen acknowledges funding from the Georgia Research Alliance and the Canada Excellence Research Chair (CERC) program.

## References

- [1] D. Polya, L. Charlet, Environmental science: rising arsenic risk? *Nat. Geosci.* **2009**, *2*, 383. doi:10.1038/NGEO537
- [2] M. L. Polizzotto, B. D. Kocar, S. G. Benner, M. Sampson, S. Fendorf, Near-surface wetland sediments as a source of arsenic release to ground water in Asia. *Nature* **2008**, *454*, 505. doi:10.1038/NATURE07093
- [3] C. F. Harvey, C. H. Swartz, A. B. M. Badruzzaman, N. Keon-Blute, W. Yu, M. A. Ali, J. Jay, R. Beckie, V. Niedan, D. Brabander, P. M. Oates, K. N. Ashfaq, S. Islam, H. F. Hemond, M. F. Ahmed, Arsenic mobility and groundwater extraction in Bangladesh. *Science* **2002**, *298*, 1602. doi:10.1126/SCIENCE.1076978
- [4] K. S. Savage, T. N. Tingle, P. A. O'Day, G. A. Waychunas, D. K. Bird, Arsenic speciation in pyrite and secondary weathering phases, mother lode gold district, tuolumne county, california. *Appl. Geochem.* **2000**, *15*, 1219. doi:10.1016/S0883-2927(99)00115-8
- [5] M. Wolthers, L. Charlet, C. H. van Der Weijden, P. R. van der Linde, D. Rickard, Arsenic mobility in the ambient sulfidic environment: Sorption of arsenic(V) and arsenic(III) onto disordered mackinawite. *Geochim. Cosmochim. Acta* **2005**, *69*, 3483. doi:10.1016/J.GCA.2005.03.003
- [6] B. C. Bostick, S. Fendorf, Arsenite sorption on troilite (FeS) and pyrite (FeS<sub>2</sub>). *Geochim. Cosmochim. Acta* **2003**, *67*, 909. doi:10.1016/S0016-7037(02)01170-5
- [7] T. J. Gallegos, S. P. Hyun, K. F. Hayes, Spectroscopic investigation of the uptake of arsenite from solution by synthetic mackinawite. *Environ. Sci. Technol.* **2007**, *41*, 7781. doi:10.1021/ES070613C
- [8] J. A. Saunders, M. K. Lee, M. Shamsudduha, P. Dhakal, A. Uddin, M. T. Chowdury, K. M. Ahmed, Geochemistry and mineralogy of arsenic in (natural) anaerobic groundwaters. *Appl. Geochem.* **2008**, *23*, 3205. doi:10.1016/J.APGEOCHEM.2008.07.002
- [9] C. F. Harvey, K. N. Ashfaq, W. Yu, A. B. M. Badruzzaman, M. A. Ali, P. M. Oates, H. A. Michael, R. B. Neumann, R. Beckie, S. Islam, M. F. Ahmed, Groundwater dynamics and arsenic contamination in bangladesh. *Chem. Geol.* **2006**, *228*, 112. doi:10.1016/J.CHEMGEO.2005.11.025
- [10] R. T. Wilkin, R. G. Ford, Arsenic solid-phase partitioning in reducing sediments of a contaminated wetland. *Chem. Geol.* **2006**, *228*, 156. doi:10.1016/J.CHEMGEO.2005.11.022
- [11] P. A. O'Day, D. Vlassopoulos, R. Root, N. Rivera, The influence of sulfur and iron on dissolved arsenic concentrations in the shallow subsurface under changing redox conditions. *Proc. Natl. Acad. Sci. USA* **2004**, *101*, 13703. doi:10.1073/PNAS.0402775101
- [12] B. C. Bostick, C. Chen, S. Fendorf, Arsenite retention mechanisms within estuarine sediments of Pescadero, CA. *Environ. Sci. Technol.* **2004**, *38*, 3299. doi:10.1021/ES035006D
- [13] M. F. Kirk, E. E. Roden, L. J. Crossey, A. J. Brealey, M. N. Spilde, Experimental analysis of arsenic precipitation during microbial sulfate and iron reduction in model aquifer sediment reactors. *Geochim. Cosmochim. Acta* **2010**, *74*, 2538. doi:10.1016/J.GCA.2010.02.002
- [14] B. D. Kocar, T. Borch, S. Fendorf, Arsenic repartitioning during biogenic sulfidization and transformation of ferrihydrite. *Geochim. Cosmochim. Acta* **2010**, *74*, 980. doi:10.1016/J.GCA.2009.10.023
- [15] E. D. Burton, S. G. Johnston, R. T. Bush, Microbial sulfidogenesis in ferrihydrite-rich environments: effects on iron mineralogy and arsenic mobility. *Geochim. Cosmochim. Acta* **2011**, *75*, 3072. doi:10.1016/J.GCA.2011.03.001
- [16] S. L. Saalfeld, B. C. Bostick, Changes in iron, sulfur, and arsenic speciation associated with bacterial sulfate reduction in ferrihydrite-rich systems. *Environ. Sci. Technol.* **2009**, *43*, 8787. doi:10.1021/ES901651K
- [17] T. J. Gallegos, Y.-S. Han, K. F. Hayes, Model predictions of realgar precipitation by reaction of As<sup>III</sup> with synthetic mackinawite under anoxic conditions. *Environ. Sci. Technol.* **2008**, *42*, 9338. doi:10.1021/ES801669G
- [18] E. Suess, A. C. Scheinost, B. C. Bostick, B. J. Merkel, D. Wallschläger, B. Planer-Friedrich, Discrimination of thioarsenites and thioarsenates by X-ray absorption spectroscopy. *Anal. Chem.* **2009**, *81*, 8318. doi:10.1021/AC901094B
- [19] F. Wang, A. Tessier, Polysulfide and metal speciation in sediment porewaters of freshwater lakes. *Environ. Sci. Technol.* **2009**, *43*, 7252. doi:10.1021/ES8034973
- [20] R. M. Couture, C. Gobeil, A. Tessier, Arsenic, iron and sulfur co-diagenesis in lake sediments. *Geochim. Cosmochim. Acta* **2010**, *74*, 1238. doi:10.1016/J.GCA.2009.11.028
- [21] P. Langner, C. Mikutta, R. Kretzschmar, Arsenic sequestration by organic sulphur in peat. *Nat. Geosci.* **2012**, *5*, 66. doi:10.1038/NGEO1329
- [22] M. Hoffmann, C. Mikutta, R. Kretzschmar, Bisulfide reaction with natural organic matter enhances arsenite sorption: insights from x-ray absorption spectroscopy. *Environ. Sci. Technol.* **2012**, *46*, 11788. doi:10.1021/ES302590X
- [23] J. P. Werne, T. W. Lyons, D. J. Hollander, S. Schouten, E. C. Hopmans, J. S. Sinninghe Damsté, Investigating pathways of diagenetic organic matter sulfurization using compound-specific sulfur isotope analysis. *Geochim. Cosmochim. Acta* **2008**, *72*, 3489. doi:10.1016/J.GCA.2008.04.033
- [24] M. Yücel, S. K. Kononov, T. S. Moore, C. P. Janzen, G. W. Luther III, Sulfur speciation in the upper black sea sediments. *Chem. Geol.* **2010**, *269*, 364. doi:10.1016/J.CHEMGEO.2009.10.010
- [25] N. R. Urban, K. Ernst, S. Bernasconi, Addition of sulfur to organic matter during early diagenesis of lake sediments. *Geochim. Cosmochim. Acta* **1999**, *63*, 837. doi:10.1016/S0016-7037(98)00306-8
- [26] R. M. Couture, B. Shafei, P. Van Cappellen, A. Tessier, C. Gobeil, Non-steady state modeling of arsenic diagenesis in lake sediments. *Environ. Sci. Technol.* **2010**, *44*, 197. doi:10.1021/ES902077Q
- [27] C. Pallud, C. Meile, A. M. Laverman, J. Abell, P. Van Cappellen, The use of flow-through sediment reactors in biogeochemical kinetics: methodology and examples of applications. *Mar. Chem.* **2007**, *106*, 256. doi:10.1016/J.MARCHEM.2006.12.011
- [28] D. Fortin, G. G. Leppard, A. Tessier, Characteristics of lacustrine diagenetic iron oxyhydroxide. *Geochim. Cosmochim. Acta* **1993**, *57*, 4391. doi:10.1016/0016-7037(93)90490-N
- [29] S. G. Benner, C. M. Hansel, B. W. Wielinga, T. M. Barber, S. Fendorf, Reductive dissolution and biomineralization of iron hydroxide under dynamic flow conditions. *Environ. Sci. Technol.* **2002**, *36*, 1705. doi:10.1021/ES0156441
- [30] F. Wang, A. Tessier, J. Buffle, Voltammetric determination of elemental sulfur in pore waters. *Limnol. Oceanogr.* **1998**, *43*, 1353. doi:10.4319/LO.1998.43.6.1353
- [31] B. Planer-Friedrich, D. Wallschläger, A critical investigation of hydride generation-based arsenic speciation in sulfidic waters. *Environ. Sci. Technol.* **2009**, *43*, 5007. doi:10.1021/ES900111Z
- [32] D. G. Beak, R. T. Wilkin, R. G. Ford, S. D. Kelly, Examination of arsenic speciation in sulfidic solutions using X-ray absorption spectroscopy. *Environ. Sci. Technol.* **2008**, *42*, 1643. doi:10.1021/ES071858S
- [33] D. Wallschläger, J. London, Determination of methylated arsenic-sulfur compounds in groundwater. *Environ. Sci. Technol.* **2008**, *42*, 228. doi:10.1021/ES0707815
- [34] B. Ravel, M. Newville, Athena, artemis, hephaestus: data analysis for X-ray absorption spectroscopy using IFEFFIT. *J. Synchrotron Radiat.* **2005**, *12*, 537. doi:10.1107/S0909049505012719
- [35] D. Wallschläger, C. J. Stacey, Determination of (oxy)thioarsenates in sulfidic waters. *Anal. Chem.* **2007**, *79*, 3873. doi:10.1021/AC070061G
- [36] G. R. Helz, J. A. Tossell, J. M. Charnock, R. A. D. Patrick, D. J. Vaughan, D. Garner, Oligomerization in As<sup>III</sup> sulfide solutions: theoretical constraints and spectroscopic evidence. *Geochim. Cosmochim. Acta* **1995**, *59*, 4591. doi:10.1016/0016-7037(95)00330-4
- [37] J. James-Smith, J. Cauzid, D. Testemale, W. H. Liu, J. L. Hazemann, O. Proux, B. Etschmann, P. Philippot, D. Banks, P. Williams, J. Brugger, Arsenic speciation in fluid inclusions using micro-beam X-ray absorption spectroscopy. *Am. Mineral.* **2010**, *95*, 921. doi:10.2138/AM.2010.3411

- [38] R.-M. Couture, J. C. Rose, N. Kumar, K. Mitchell, D. Wallschläger, P. Van Cappellen, Sorption of arsenite, arsenate and thioarsenates to iron oxides and iron sulfides: a kinetic and spectroscopic investigation. *Environ. Sci. Technol.* **2013**, *47*, 5652. doi:10.1021/ES3049724
- [39] A. Manceau, K. L. Nagy, Quantitative analysis of sulfur functional groups in natural organic matter by xanes spectroscopy. *Geochim. Cosmochim. Acta* **2012**, *99*, 206. doi:10.1016/J.GCA.2012.09.033
- [40] Y. P. Hsieh, Y. N. Shieh, Analysis of reduced inorganic sulfur by diffusion methods: Improved apparatus and evaluation for sulfur isotopic studies. *Chem. Geol.* **1997**, *137*, 255. doi:10.1016/S0009-2541(96)00159-3
- [41] E. D. Burton, L. A. Sullivan, R. T. Bush, S. G. Johnston, A. F. Keene, A simple and inexpensive chromium-reducible sulfur method for acid-sulfate soils. *Appl. Geochem.* **2008**, *23*, 2759. doi:10.1016/J.APGeochem.2008.07.007
- [42] D. L. Parkhurst, C. A. J. Apello, *User's guide to PHREEQC (Version 2) : a computer program for speciation, batch-reaction, one-dimensional transport, and inverse geochemical calculations. Water-Resources Investigations Report 99-4259* **1999** (US Geological Survey: Denver, CO). Available at <http://pubs.er.usgs.gov/publication/wri994259> [Verified 28 June 2013].
- [43] D. Canfield, E. Kristensen, B. Thamdrup, *Advances in Marine Biology: Aquatic Geomicrobiology*, vol. 48 (Eds AJ Southward, PA Tyler, CM Young, LA Fuiman) **2005** (Elsevier Academic Press: San Diego, CA).
- [44] E. D. Burton, R. T. Bush, S. G. Johnston, L. A. Sullivan, A. F. Keene, Sulfur biogeochemical cycling and novel Fe-S mineralization pathways in a tidally re-flooded wetland. *Geochim. Cosmochim. Acta* **2011**, *75*, 3434. doi:10.1016/J.GCA.2011.03.020
- [45] S. W. Poulton, M. D. Krom, R. Raiswell, A revised scheme for the reactivity of iron (oxyhydr)oxide minerals towards dissolved sulfide. *Geochim. Cosmochim. Acta* **2004**, *68*, 3703. doi:10.1016/J.GCA.2004.03.012
- [46] J. P. Werne, D. J. Hollander, T. W. Lyons, J. S. Sinninghe Damsté, Organic sulfur biogeochemistry: recent advances and future research directions. *Spec. Pap. Geol. Soc. Am.* **2004**, *379*, 135.
- [47] G. R. Helz, J. A. Tossell, Thermodynamic model for arsenic speciation in sulfidic waters: a novel use of ab initio computations. *Geochim. Cosmochim. Acta* **2008**, *72*, 4457. doi:10.1016/J.GCA.2008.06.018
- [48] D. Solomon, J. Lehmann, M. Tekalign, F. Fritzsche, W. Zech, Sulfur fractions in particle-size separates of the sub-humid ethiopian highlands as influenced by land use changes. *Geoderma* **2001**, *102*, 41. doi:10.1016/S0016-7061(00)00103-8
- [49] J. r. Prietzel, A. Botzaki, N. Tyufekchieva, M. Brettholle, J. r. Thieme, W. Klysubun, Sulfur speciation in soil by s k-edge xanes spectroscopy: comparison of spectral deconvolution and linear combination fitting. *Environ. Sci. Technol.* **2011**, *45*, 2878. doi:10.1021/ES102180A
- [50] B. Morgan, E. D. Burton, A. W. Rate, Iron monosulfide enrichment and the presence of organosulfur in eutrophic estuarine sediments. *Chem. Geol.* **2012**, *296-297*, 119. doi:10.1016/J.CHEMGEO.2011.12.005
- [51] M. L. Farquhar, J. M. Charnock, F. R. Livens, D. J. Vaughan, Mechanisms of arsenic uptake from aqueous solution by interaction with goethite, lepidocrocite, mackinawite, and pyrite: an X-ray absorption spectroscopy study. *Environ. Sci. Technol.* **2002**, *36*, 1757. doi:10.1021/ES010216G
- [52] B. Planer-Friedrich, E. Suess, A. C. Scheinost, D. Wallschläger, Arsenic speciation in sulfidic waters: reconciling contradictory spectroscopic and chromatographic evidence. *Anal. Chem.* **2010**, *82*, 10228. doi:10.1021/AC1024717
- [53] R.-M. Couture, P. Van Cappellen, Reassessing the role of sulfur geochemistry on arsenic speciation in reducing environments. *J. Hazard. Mater.* **2011**, *189*, 647. doi:10.1016/J.JHAZMAT.2011.02.029
- [54] E. Suess, B. Planer-Friedrich, Thioarsenate formation upon dissolution of orpiment and arsenopyrite. *Chemosphere* **2012**, *89*, 1390. doi:10.1016/J.CHEMOSPHERE.2012.05.109
- [55] E. Suess, D. Wallschläger, B. Planer-Friedrich, Stabilization of thioarsenates in iron-rich waters. *Chemosphere* **2011**, *83*, 1524. doi:10.1016/J.CHEMOSPHERE.2011.01.045
- [56] B. Planer-Friedrich, D. Franke, B. Merkel, D. Wallschläger, Acute toxicity of thioarsenates to *Vibrio fischeri*. *Environ. Toxicol. Chem.* **2008**, *27*, 2027. doi:10.1897/07-633.1
- [57] R.-M. Couture, A. Sekowska, G. Fang, A. Danchin, Linking selenium biogeochemistry to the sulfur-dependent biological detoxification of arsenic. *Environ. Microbiol.* **2012**, *14*, 1612. doi:10.1111/J.1462-2920.2012.02758.X